45th AIAA Aerospace Sciences Meeting and Exhibit
8-11 January 2007, Reno, Nevada

AIAA 2007 - 0723

LES and DES simulations for aircraft design

Frederic Chalot[*], Vincent Levasseur[†], Michel Mallet[*], Gabriel Petit[*], Nicolas Reau[*]
Dassault Aviation, 78 quai Dassault, 92552 Saint Cloud, France

The paper first describes developments performed to achieve an accurate and efficient simulation capacity using turbulence models based on the LES and DES approaches. The development is performed within the industrial code used at Dassault for the aerodynamics design of both military aircraft and business jets. The issues of subgrid scale implementation and wall treatment approaches are addressed. The paper then presents industrial applications performed at Dassault related to aerodynamic design. Examples demonstrate the impact of LES and DES on key design issues where complex flow features are present.

Nomenclature

C_p	=	pressure coefficient
k	=	turbulent kinetic energy
ε	=	turbulent energy dissipation
DC(θ)	=	distortion coefficient based on θ deg. sector
K_θ	=	circumferential distortion coefficient

Abbreviations :

CEP	Compressor Entry Plane
DES	Detached Eddy Simulation
DDES	Delayed Detached Eddy Simulation
GIS	Grid Induced Separation
LES	Large Eddy Simulation
RANS	Reynolds Averaged Navier Stokes
RMS	Root Mean Square
SAS	Scale Adaptive Simulation
UAV	Unmanned Air Vehicle

I. Introduction

Reynolds Averaged Navier Stokes (RANS) simulations have reached a mature and validated capacity[1,2], their range of application is well identified and they are used routinely for aerodynamic design. A detailed review of the state of the art in CFD for industrial aerodynamics can be found in[3]. However, RANS models lack accuracy for flows with strong non equilibrium and high anisotropy. Such flow features are observed for example in the presence of large recirculating flows. Related aerodynamic design problems include the study of off-design points for civil aircraft like post stall or strong buffet, the analysis of flows associated with unconventional shapes dictated by stealth, or flow with fluidic control devices.
Improved turbulence modeling can be obtained by using Large Eddy Simulation (LES). For a long time, LES was perceived as a modeling technology that would not have an impact on aerodynamic design in

[*] Advanced Aerodynamics and Aeroacoustics (DTIAE/AERAV).
[†] Advanced Aerodynamics and Aeroacoustics (DTIAE/AERAV) and University of Paris.

industry before many years[4]. This view has changed significantly. Part of this change is due to the Detached Eddy Simulation (DES) approach[4,5] that proposes a way to deal with the near wall flow.
In the first part of this paper, the developments associated to the integration of LES and DES approaches are described. The influence of the subgrid model and the wall treatment are discussed.
In the second part, a number of applications are presented. They illustrate design problems where unsteady simulations have been found to be relevant both for military aircraft (including UAVs) and business jets. Comparisons between LES and DES results are performed.

II. Development and implementation of LES and DES models

Initial work was dedicated to establishing the feasibility of LES associated to second order accurate unstructured schemes based on the Galerkin least squares (GLS) stabilized finite element discretization[6]. The reference Smagorinsky model and a selective subgrid scale model were implemented. This initial work was based on explicit time integration using Runge Kutta schemes with a time consistent GLS operator[7, 8].

Recent work on LES has been devoted to the study of novel subgrid scale models based on a variational multiscale approach following ideas proposed by Hughes[9, 10]. The formulation implemented is a filtered variant[11, 12]. The simulation also uses an implicit time integration with dual time stepping. Implicit Runge Kutta, backward difference or trapezoidal schemes can be applied.

Two versions of the DES approach have also been implemented and are currently used in the design process. The first version is based on the Spalart-Allmaras model and the second version on the k-ε SST two equation turbulence model.

The constants of Spalart and k-ε DES are calibrated so that the far field models correctly reproduce the energy transfer. This calibration is performed using the Decay of Homogeneous Isotropic Turbulence test case. The computation is performed on a 51^3 box. DES results are compared to LES results and the constants are selected to reach the $k^{-5/3}$ slope. This is illustrated in Figure 1 where the decrease of kinetic energy is presented when using different DES and LES sub-scale viscosity models.

One difficulty associated to the DES approach is the behavior of the switch between the RANS model and the LES mode. In the near wall region the model should select the RANS mode. However, when the mesh is too fine in the longitudinal direction, the original DES approach will reduce the RANS viscosity. This modeled stress depletion can yield flow separation. This phenomena is usually called "Grid Induced Separation" (GIS). Near wall treatments have been proposed to avoid this problem: DDES formulation is used for Spalart-Allmaras DES while Menter SST function is accurate for k-ε.

The DDES model is outlined in the following equations.

$$\frac{D}{Dt}\rho\tilde{\nu} = c_{b1}\tilde{S}\rho\tilde{\nu} - \rho c_{w1} f_w \left(\frac{\tilde{\nu}}{d}\right)^2 + \frac{1}{\sigma}\left(\nabla.(\mu+\rho\tilde{\nu})\nabla\rho\tilde{\nu} + c_{b2}\rho(\nabla\tilde{\nu})^2\right)$$

$$\tilde{d} = d - f_d \max(0, d - C_{des}\Delta)$$

$$f_d = 1 - \tanh\left([8r_d]^3\right) \text{ and } r_d = \frac{\tilde{\upsilon}}{\sqrt{U_{i,j}U_{i,j}}\kappa^2 d^2}$$

Parameter r_d is equal to 1 in the logarithmic zone et drops rapidly to 0 above. In the viscous layer, r_d is driven by molecular viscosity. The F_d blending function therefore goes to 0 in near-wall zone improving the boundary-layer treatment.

DES based on the k-ε model is already available in the literature (see e.g. Travin[13]). The modification of the basic k-ε consists in the following modification of the destruction term in the k-equation :

$$D_k = \rho k^{3/2} / \tilde{l} \quad \text{with } \tilde{l} = \min(l_{k-\varepsilon}, \frac{C_{DES}\Delta}{1-F_2})$$

F_2 is a SST blending function proposed by Menter[14] usually applied to correct eddy-viscosity in the boundary layer under adverse pressure gradient.

These wall treatments have been validated using a generic flat plate flow test case. The mesh is fine in the longitudinal direction. Results are presented on Figure 2 where longitudinal velocity profiles in wall

variables obtained using standard and modified DES models are compared to reference profiles. The standard DES models fail. The DDES modification and Menter formulation both lead to acceptable results.

III. Applications

A. Shear layer with mixing enhancement

This application is related to flow control techniques: a jet is injected perpendicular to a shear layer to trigger mixing enhancement. This configuration was studied in[8] with a continuous jet. The configuration and flow structure are presented in Figure 3. Mean Mach number profiles through the shear layer downstream of the injector are presented in Figure 4. Experimental results are compared to both RANS and LES results. The RANS model used is a k-ε model. The LES approach leads to a large improvement of results when the perpendicular jet is active. The feasibility of flow control strategies is usually limited by the amount of air available for perpendicular injection. One way to reduce the flow required is to use pulsed jets. LES simulation was performed to assess the impact on the mixing enhancement of the fact that the jet is pulsed. The mass flow rate is divided by two. The jet frequency is chosen to match frequency of the main shear layer instability. The experimental continuous jet and LES pulsed jet profiles are compared on Figure 5. Similar mixing enhancement is observed. This demonstrates the possibility to reduce the flaw rate. However, no increase in the mixing efficiency is produced by the matching of the shear layer and jet frequencies.

B. Weapon bays

The design of weapon bays is one of the challenges associated to the aerodynamic design of stealth aircraft. Indeed, large amplitude aerodynamic loads develop in an open bay leading to structural vibrations that could endanger the integrity of the aircraft. Since Rossiter's work (1964), the aeroacoustic coupling is known to induce very strong periodic pressure fluctuations. The sum of the so-called Rossiter modes and of the broad band noise associated with the shear layer create extremely high vibration loads. Accurate aerodynamic predictions will avoid structural over-design with an associated weight penalty or reduced structural life due to fatigue. Efficient palliatives can greatly reduce the loads, reliable simulation capacities are instrumental for their design.

Numerical computations have been carried out based on a generic configuration experimented by QinetiQ in the ARA Bedford and DERA Bedford wind tunnels[15], at Mach number equal to 0.85. The configuration considered and mesh used for the LES computations are presented on Figure 6. LES have proven to be a valuable tool for the prediction of cavity flows: a very good agreement is obtained with experiments in terms of pressure fluctuations measured at the ceiling of the cavity. The Rossiter modes are accurately predicted in both frequency and amplitude as can be seen in Figure 7 and 8. Very good results are also obtained using a DES approach - see Figure 9. This configuration is not very sensitive to the accuracy the prediction of the incoming boundary layer: it is sufficient to have a correct prediction of the boundary layer thickness at the inflow of the cavity. In that sense, this configuration is well suited for LES simulation.

Two passive control strategies are then investigated: the rod-in-crossflow and the flat-top spoiler. Both devices lead to an overall 3-4 dB pressure fluctuations reduction. Looking at the mean field, Figure 10, both palliatives have a common effect which is simply an upward deflection of the shear layer. The impact of turbulent vortices on the downstream corner of the cavity is therefore lowered, providing one explanation of the pressure fluctuation suppression. Yet, looking closely at the physical mechanisms highlights two distinct behavior. The streamwise evolution of pressure coefficients, Figure 11, shows that both devices increase the Kp-plateau length, this confirms the primarily deflection effect. However, the cavity undergoes much more important load while controlling with the spoiler. Actually, on the one hand the spoiler seems to affect the Rossiter modes production mechanisms, while maintaining a high pressure level. On the other hand, the rod provides sharp peaks but lower the global pressure level. This can be seen for example on Figure12, where the acoustic spectra for both control devices is displayed. One can also notice the very good agreement with experiments. Stanek and co-workers[15] stated that the rod provides a high-frequency forcing through the induced vortex shedding, modifying the hydrodynamics stability properties of the mean flow. Finally the turbulent vortices of the flow are presented on Figure 13. Very different structures are observed. The perturbation due to the rod generates small-scales turbulence while the spoiler produces large bidimensional structures. For a more detailed analysis of the physical mechanisms the reader is referred to[16, 17].

As a conclusion, Large-Eddy Simulations produces results in very good agreement with experimental data but also allows a detailed insight into the complex mechanisms produced by the subsonic compressible flow over a cavity. Detached-Eddy Simulation are now performed in an design-oriented goal, to predict weapon release from the cavity. Uunstructured mesh approaches are well suited for this type of geometrically complex configurations that include the door, palliative device and weapon.

C. Curved air inlets

Curved air inlet are needed to shield the Compressor Entry Plane (CEP) of stealth aircraft, in particular strike UAVs. An essential design objective is to reduce the total length of the aircraft, this can be achieved by a reduction of the length of the diffuser. This requires high curvature and can lead to very distorted flows. The design must keep pressure recovery and static and dynamic flow distortion at an acceptable level. Distortion coefficients DC(θ) and K_θ are predicted. Standard RANS models yield poor predictions of the recirculation areas inside the inlet. DES type models improve flow prediction and also predicts valuable information on the unsteadiness of the flow reaching the CEP.

One great issue that hybrid unsteady methods have to deal with in such constraint flow, is to reach separation point location with accuracy. When using only the academic RANS/DES switch, phenomenon of GIS (Grid Induced Separation) is commonly observed, leading to non-physical results. In order to prevent such a behavior, the near wall formulations described above are relevant. The impact of these improved DES models is clear on the analysis of the generic S-Duct[19, 20] considered here. The unstructured mesh is presented on Figure 14, it contains $1.6.10^6$ points. Instantaneous flow fields are presented on Figure 15 and 16 and illustrate the complexity of the flow. A comparison between measured and computed mean Mach number at the Compressor Entry Plane (C.E.P) is presented on Figure 16. Good agreement is obtained. Beyond unsteady flow field characteristics, DES computations also improve the prediction of mean flow due to the mixing enhancement specially for total pressure loss in the inlet: this can be seen in the table below where total pressure recovery and distortion results are summarized.

	Pressure recovery	**DC60**
Experiment	0.971	0.358
Steady Spalart	0.9815	0.479
Steady k-ε	0.9816	0.4781
Spalart DES	0.978	0.377
k-ε DES	0.9804	0.403

Mean flow characteristics: Steady vs. Unsteady results. DC60 represents the weight of the worst 60° field in the CEP in terms of distortion.

Additional informations obtained by using DES are dynamic distortion (mean of instantaneous distortion) which can be very different of the computed mean flow distortion, and RMS values in the CEP to prevent compressor blade fatigue.

The analysis described above is currently being applied to the study of highly curved U inlets. Design of such inlets with control devices, viz. Mechanical or Fluidic Vortex-Generators, is also an important application.

D. Wing profile

The flow considered displays a recirculation area near the trailing edge. The mesh and the average velocity field are presented on Figure 17, average velocity profiles at several locations through the recirculation are presented in Figure 18 where LES and RANS results are compared. The LES computation was run with wall functions. This represents a first attempt at dealing with this type of configuration. An improved prediction of the small area of recirculating flow can be observed with the LES approach.

E. Airbrake design

The design of airbrakes is a typical example of a design problem that extends beyond the prediction of the flow at cruise conditions. The complex flow features with large recirculation represents a challenge for turbulence models. During the design of the Falcon 7X long range business jet, RANS calculations have

been performed to evaluate airbrake efficiency. A typical result is presented on Figure 19. The relative influence of the airbrake deflection on aircraft lift and drag is correctly predicted. However hinge efforts are not predicted correctly. DES results will be performed for this problem and improved results are expected.

IV. Conclusions

The development and validation work performed to achieve unsteady turbulent simulations has been described. A number of examples of applications for aerodynamic design have been presented. This illustrates the value of LES and DES approaches for the simulation of complex flows and engineering design problems where unsteady data is needed. This is the case for engine integration where engine manufactures specify allowable unsteadiness levels. This is also required when aerodynamic calculations are performed to provide input data for structural design to assess vibration levels or fatigue life.

A number of shortcomings of turbulence models are identified: the behavior of DES models in the near wall region is still not satisfactory: the problem of the "grey zone" must be addressed. The SAS model proposed by Menter and Egorov[17] is one possible answer. Innovative RANS/LES coupling can also be considered even though they are still too complex to be routinely used in industry at present. The issue of transition is also a challenge. This includes the well known transition in a laminar separation bubble. LES, possibly with a zonal approach, could bring an answer.

Future trends include the use of innovative high order numerical methods[10]. These methods are likely to have a very large impact on the type of simulations presented in this paper. It can also be anticipated that future development will benefit from continued growth of computer speed. This will be made possible by massively parallel architectures with thousands of processors[21]. This may raise implementation issues and impact the choice of algorithms.

Improved modeling and increased computer power will open new areas to simulation for design in industry. Pioneering work is already available on the study of high lift configurations[22] (also at stall or post stall), the study of wing buffet[23], wing drop[24] or maneuvering aircraft[25]. Computational Aero Acoustics (CAA) is also impacted by LES and DES simulations[26, 27], this trend will most likely be amplified in the future.

Acknowledgments

The second author was supported by a Doctoral research grant from the Ministry of Defense (DGA). Part of the work was funded under a grant by the European Commission through the DESIDER project of the 6th Framework program.

References

[1]Chalot, F., Mallet, M., "The stabilized Finite Element Method for compressible Navier Stokes simulations: review and application to aircraft design", in Finite Element Methods: 1970's and beyond, L. P. Franca (Ed.) CIMNE, Barcelona, (2004)

[2]Rostand, P., "New Generation Aerodynamic and Multidisciplinary Design Methods for FALCON Business Jets. Application to the F7X" AIAA paper 2005-5083, *23rd AIAA Applied Aerodynamics Conference*, Toronto, (2005).

[3]Chalot, F., « Industrial Aerodynamics », Encyclopaedia of Computational Mechanics, Volume 3, Wiley (2004)

[4]Spalart, P., Jou, W.H., Strelets, M. and Allmaras, S.R., "Comments on the feasibility of LES for wings and on a hybrid RANS/LES approach". Proceedings pp137-147, 1st AFSOR Int. Conf on DNS/LES, Ruston, (1997).

[5]Strelets, M., "Detached Eddy Simulation of Massively Separated Flows" AIAA paper 01-0879, *39th AIAA Aerospace Sciences Meeting and Exhibit*, Reno, (2001).

[6]Hughes, T., J., R., Mallet, M., "A New Finite Element Formulation for Computational Fluid Dynamics, III The Generalized Streamline Operator for Multidimensional Advective-Diffusive Systems", *Computer methods in applied Mechanics and Engineering,* 58, 305-328, (1986).

[7]Chalot, F., Marquez, B., Ravachol, M., Ducros, F., Nicoud F., Poinsot, Th., "A consistent Finite Element Approach to Large Eddy Simulation", *29th Fluid Dynamics conference*, AIAA 98-2652, (1998)

[8]Chalot, F., Marquez, B., Ravachol, M., Ducros, F., Poinsot, T., "Large Eddy Simulation of a Compressible Mixing Layer : Study of the mixing enhancement", *14th CFD conference*, AIAA 99-3358 (1999).

[9]Hughes, T.J.R., Mazzie, L., Jansen, K.E., "Large eddy simulation and the variational multiscale method", *Comput. Visual Sci.* 3, 47-59 (2000).

[10]Hughes, T.J.R., Calo, V.M., Scovazzi, G., «A multiscale discontinous Galerkin method», ICES Report, UT Austin (2005)
[11]Vreman, A. W., "The filtering analog of the variational multiscale method in large-eddy simulation", *Phys. Fluids* 15, L61, (2003).
[12]Levasseur, V., Sagaut, P., Chalot, F., Davroux, A., "An entropy variable based VMS/GLS method for the simulation of compressible flows on unstructured grids", *Computer methods in applied Mechanics and Engineering* 195, 1154-1179, (2006).
[13]A. Travin, M. Shur, M. Strelets, Spalart P.R., *Physical and Numerical Upgrades in the Detached Eddy Simulation of Complex turbulent Flows*, 412 EuroMech Colloquium on LES of Complex Transitional and turbulent flows, Munich, Oct.2000.
[14]Menter, F.R, Egorov, Y, "A scale adaptative simulation model using two-equation models" AIAA 2005-1095
[15]Stanek, M.J., Ross, J.A., Odedra, J. and Peto J., "High frequency acoustic suppression - the mystery of the rod-in-crossflow revealed", *41st AIAA Aerospace Sciences Meeting and Exhibit*, Reno, (2003).
[16]Levasseur, V., Sagaut, P., Mallet, M., Chalot, F., "Unstructured Large Eddy Simulations of the flow in a three-dimensional open cavity with passive control", *submitted to Computer and Fluids*
[17]Levasseur, V., "Simulation des Grandes Echelles en Eléments Finis Stabilisés: une approche Variationnelle Multi-Echelles", PhD Thesis, University of Paris, *(in French)*
[18]Spalart, P.R., Deck, S., Shur, M.L., Squires, K. D., Strelets, M. Kh., Travin, A, "A new version of Detached Eddy Simulation resistant to ambiguous grid densities", *Th. And Comp. Fluid Dyn*.
[19]Harloff, G, J, Reichert, B. A, Wellborn, S. R, " Navier-Stokes Analysis and experimental data comparison of compressible flow in a diffusing S-Duct", *AIAA- 92-2699-CP*
[20]Vuillerme, A-L, Deck, S, Chevrier, R, "Numerical simulations of the flow inside an S-shaped intake diffuser", *1st EUCASS conference, Moscou, 4-7 juillet 2005*
[21]Aftosmis, M., Berger, M., Biswas, R., Djomehri, M.J., Hood, R., Jin, H., Kiris, C., "A Detailed Performance Characterization of Columbia using Aeronautics Benchmarks and Applications" AIAA paper 2006-84, *44th AIAA Aerospace Sciences Meeting and Exhibit*, Reno, (2006).
[22]Deck, S., "Zonal-Detached-Eddy Simulation of the flow Around a High-Lift Configuration" AIAA Journal, Vol.43, No. 11, November 2005.
[23]Deck, S., "Numerical Simulation of Transonic Buffet over a Supercritical Airfoil" AIAA Journal, Vol.43, No. 7, pp1556-1566, July 2005.
[24]Forsythe, J.,R., Wodson, S.,H., "Unsteady CFD Calculations of Abrupt Wing Stall Using DES", AIAA paper 2003-0594, *41st AIAA Aerospace Sciences Meeting and Exhibit*, Reno, (2003).
[25]Forsythe, J.,R., Strang, W., Z., Squires, K., D., "Six Degree of Freedom Computation of the F-15E Entering a Spin", AIAA paper 2006-858, *44th AIAA Aerospace Sciences Meeting and Exhibit*, Reno, (2006).
[26]Shur, M., Spalart, Ph., Strelets, M., Garbaruk, A., "Further steps in LES-based Noise Prediction for Complex Jets" AIAA paper 2006-0485, *44th AIAA Aerospace Sciences Meeting and Exhibit*, Reno, (2006).
[27]Paliath, U., Morris, P., J., "Prediction of Jet Noise from Rectangular Nozzles" AIAA paper 2006-0618, *44th AIAA Aerospace Sciences Meeting and Exhibit*, Reno, (2006).

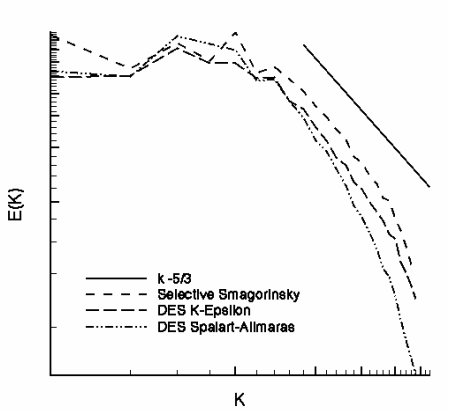

Figure 1. Decay of Homogeneous turbulence - comparison of LES and DES results

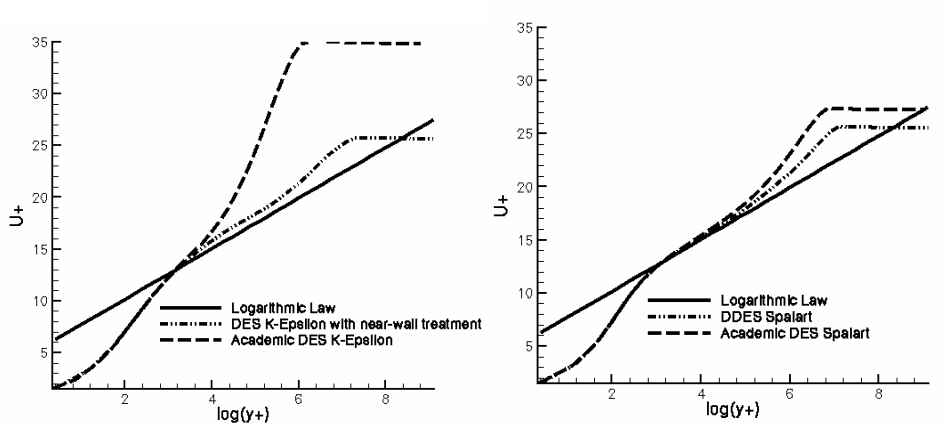

Figure 2. Flow over a flat plate - influence of the near wall model on DES results

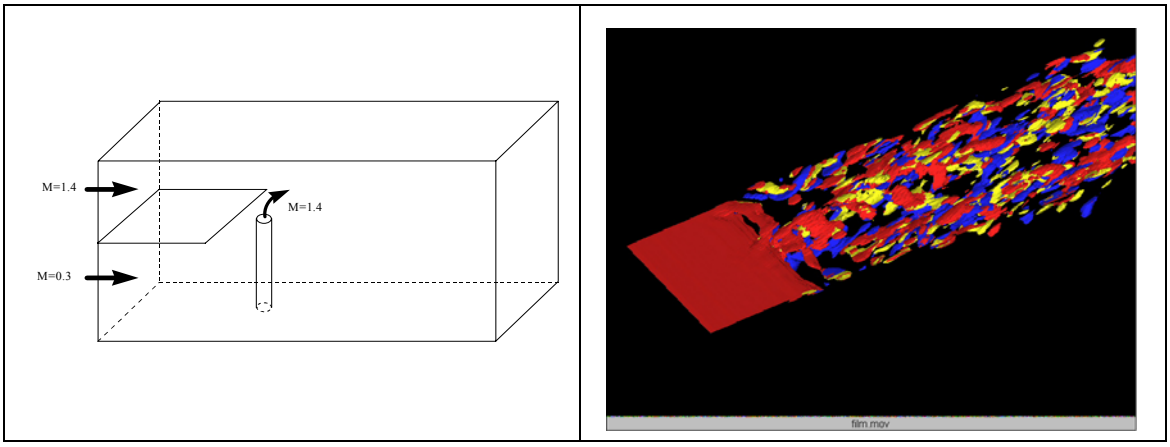

Figure 3. Shear layer with mixing enhancement - left: configuration, right: Q criteria, flow with perpendicular jet active

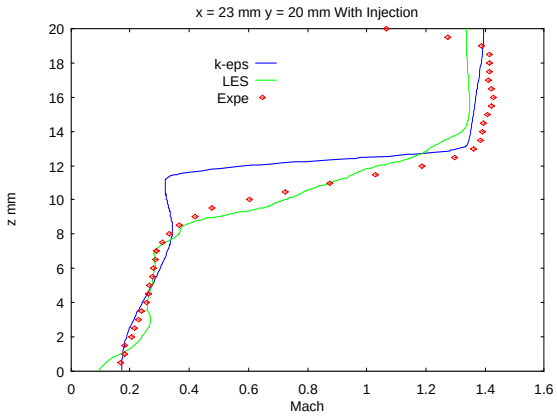

Figure 4. Shear layer with mixing enhancement - Time-averaged Mach number profile through the shear layer downstream of the injector - Comparison of LES and RANS results

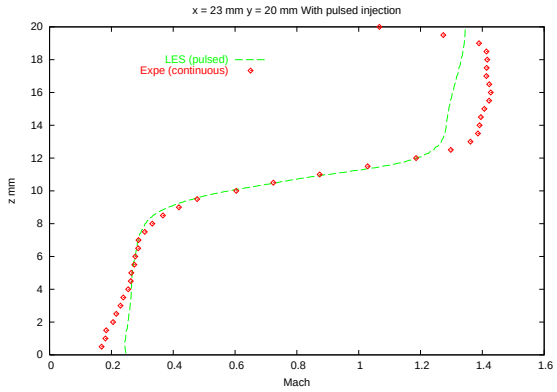

Figure 5. Shear layer with mixing enhancement - Time-averaged Mach number profile through the shear layer downstream of the injector - Comparison of continuous and pulsed blowing

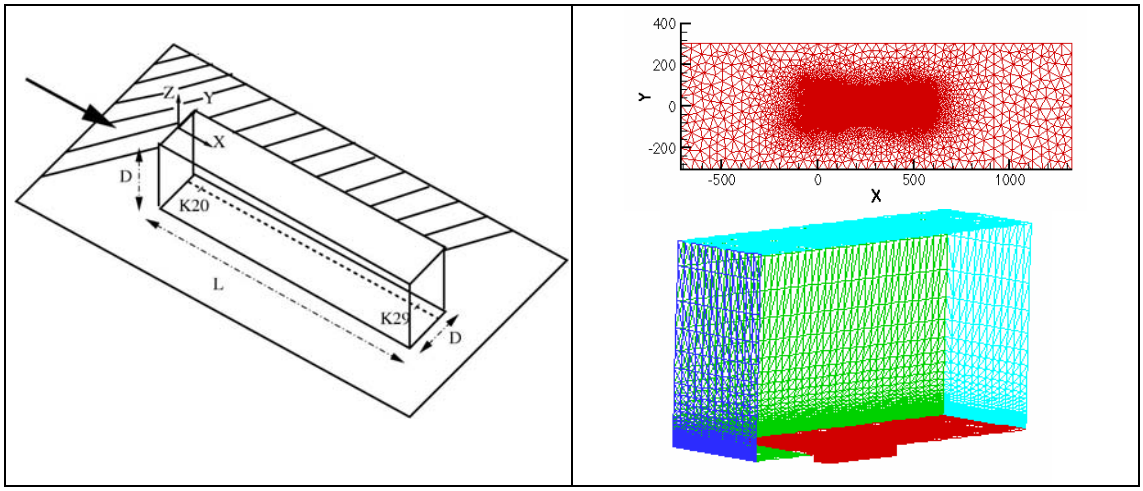

Figure 6. cavity flow - left: configuration, right: unstructured surface mesh

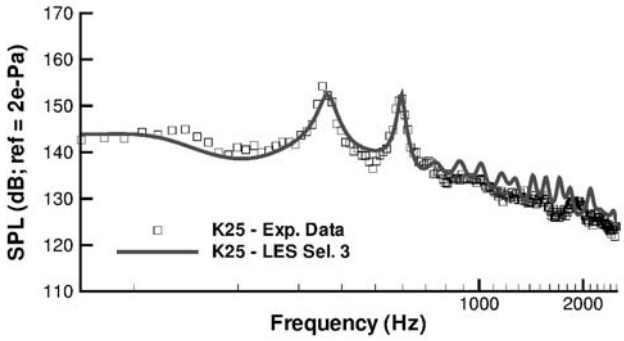

Figure 7. Acoustic spectra of LES cavity flow

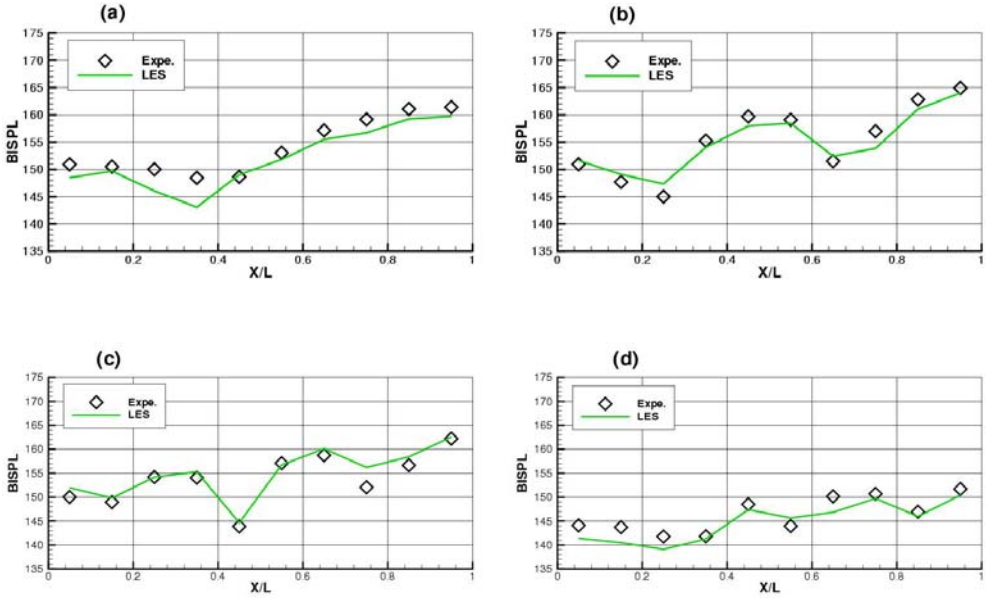

Figure 8. Band integrated sound pressure level. Energy contained in the 1st (a), 2nd (b), 3rd (c) and 4th (d) Rossiter modes

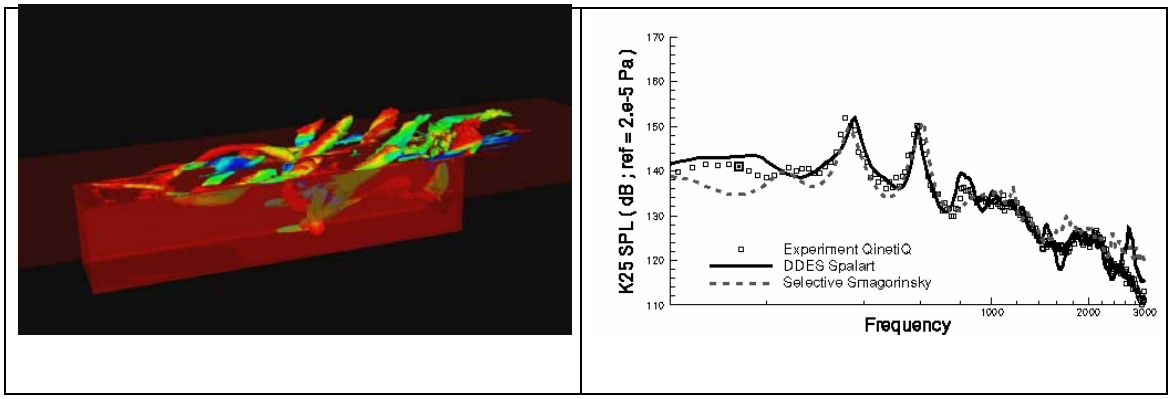

Figure 9. DES of cavity - left: flow structure, right: acoustic spectra

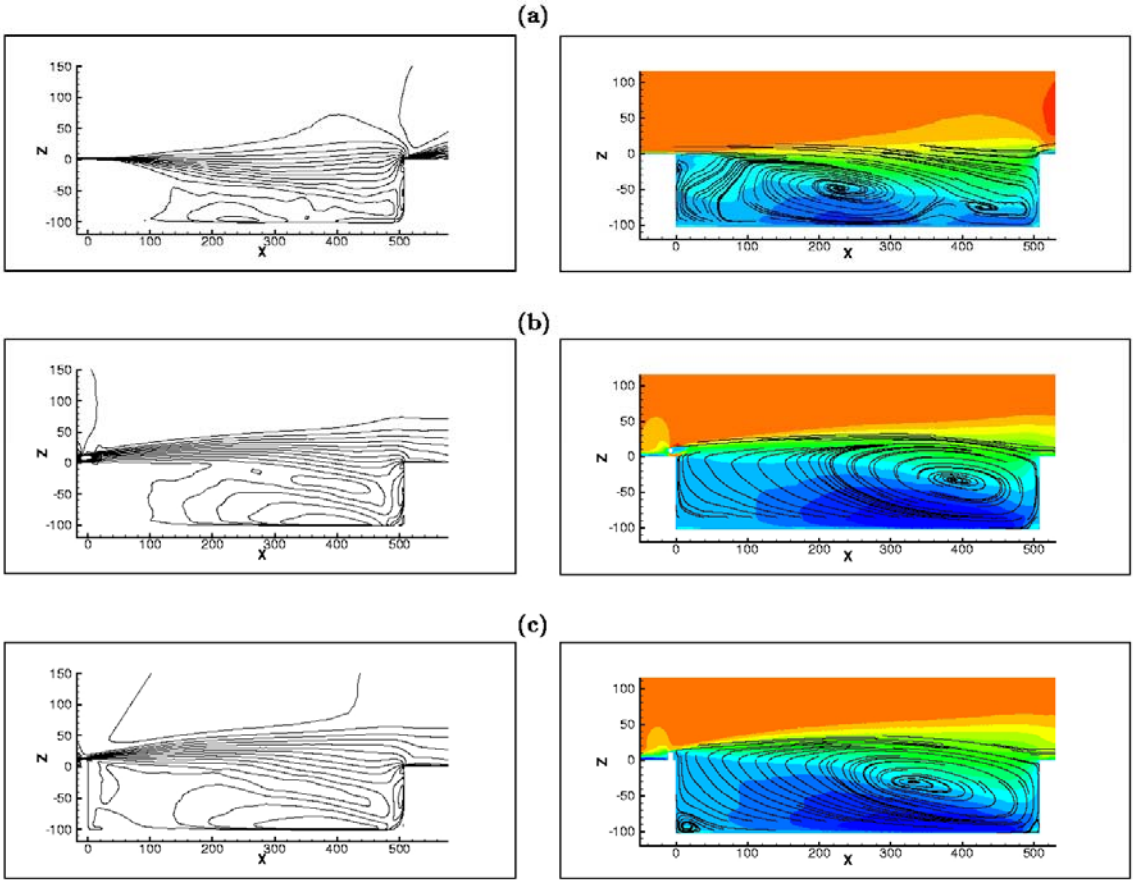

Figure 10. Isolines of Mach number (left) and streamlines of the mean field. No device (a), rod-in-crossflow (b), spoiler(c)

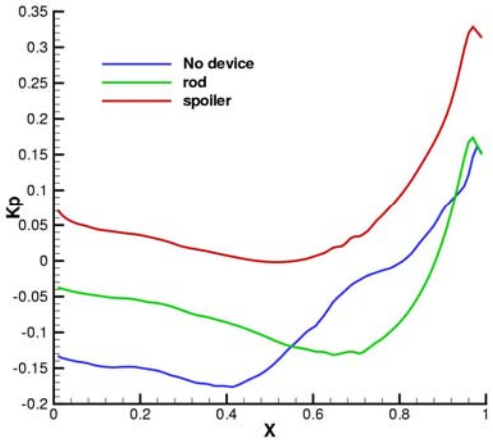

Figure 11. Streamwise evolution of pressure coefficient at the ceiling of the bay

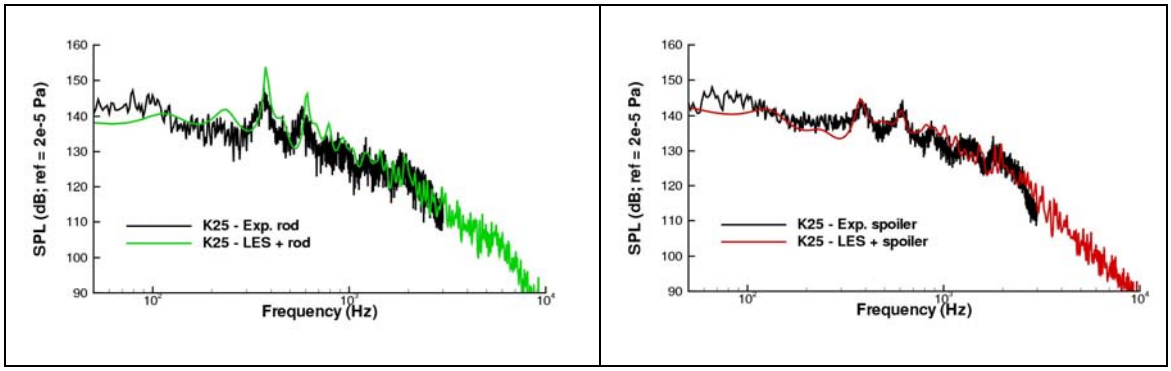

Figure 12. Comparison of measured and computed acoustic spectra for the rod (left) and spoiler (right configurations.

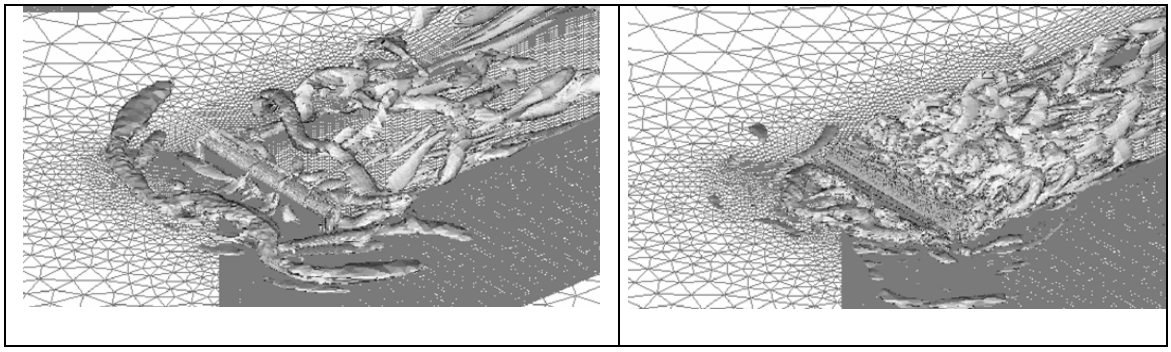

Figure 13. LES of cavity with flow control devices - comparison of spoiler(left) and rod(right)

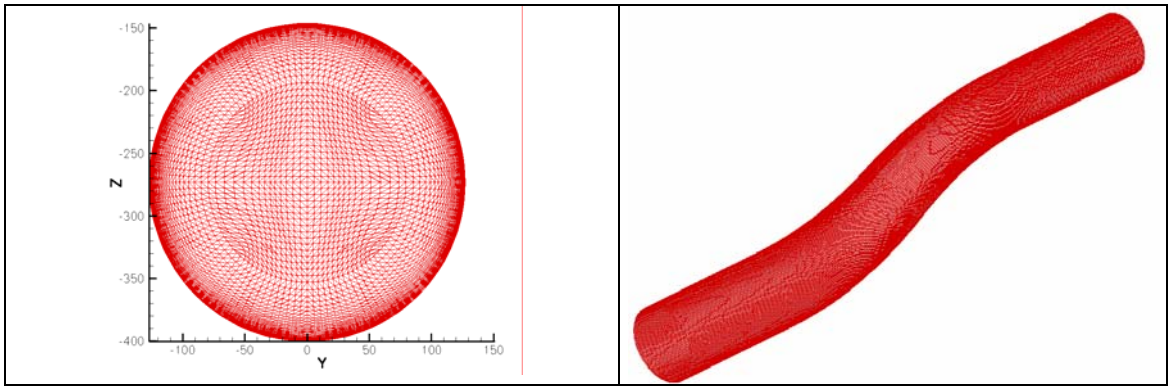

Figure 14. Unstructured mesh in an S shaped air inlet - surface mesh (left) and mesh section (right)

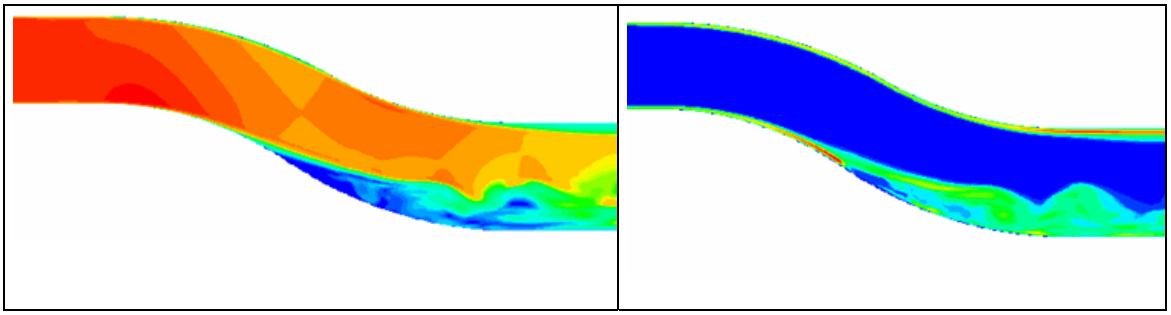

Figure 15. DES in an S shaped air inlet - Instantaneous Mach number (left) and turbulent viscosity (right)

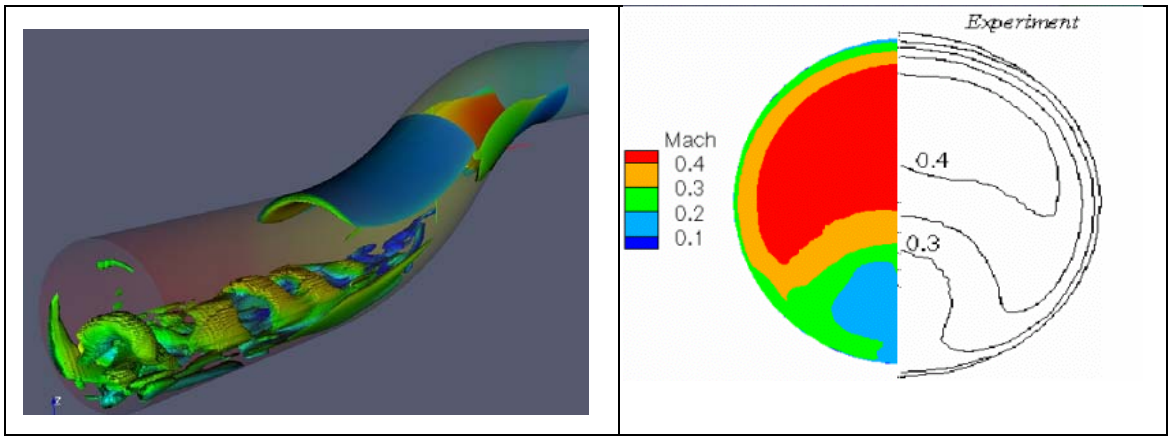

Figure 16. DES in an S shaped air inlet - Weiss Criteria(left) - Mean Mach field in the CEP (right)

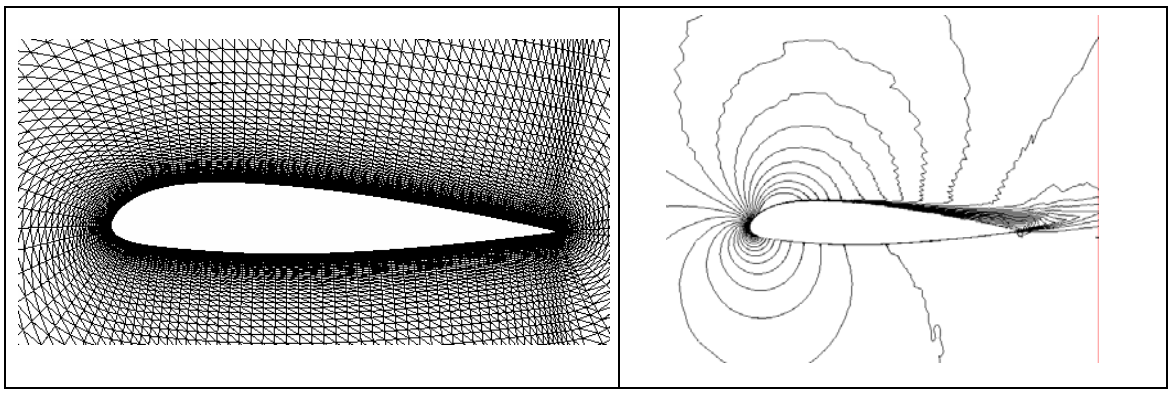

Figure 17. LES of airfoil profile - left: unstructured mesh, right: average velocity field

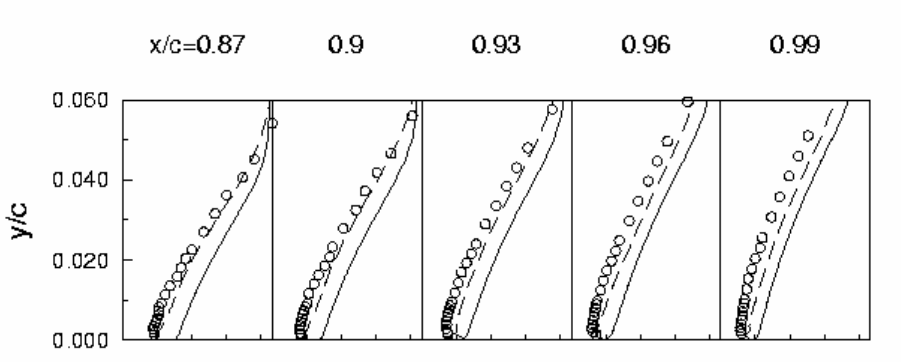

Figure 18. LES of airfoil profile - velocity profiles through recirculation (o : experiment, - - - : LES with wall functions, — : (*k*, *ε*) with wall functions)

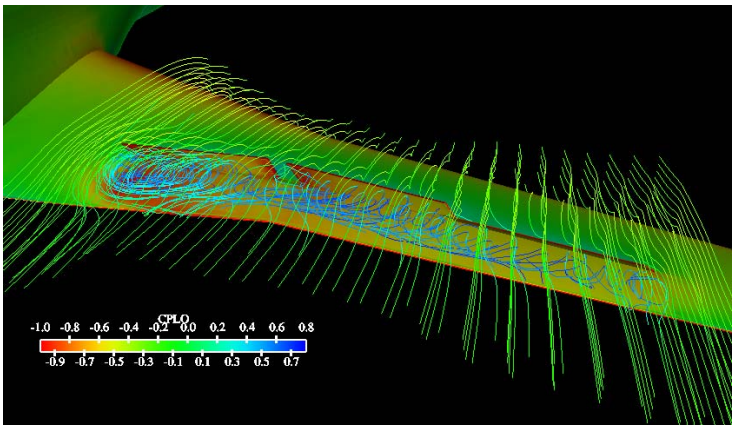

Figure 19. RANS calculation of the flow over the Falcon 7X wing with airbrakes deployed (surface pressure coefficient C_p and streamlines)